

# LOW ENERGY MUON SPIN ROTATION AND POINT CONTACT TUNNELING APPLIED TO NIOBIUM FILMS FOR SRF CAVITIES

T. Junginger<sup>\*1,2</sup>, S. Calatroni<sup>3</sup>, T. Proschka<sup>5</sup>, T. Proslie<sup>6</sup>, Z. Salman<sup>5</sup>, A. Suter<sup>5</sup>, G. Terenziani<sup>3,4</sup>, and J. Zasadzinski<sup>7</sup>

<sup>1</sup>TRIUMF Canada's National Laboratory for Particle and Nuclear Physics, Vancouver

<sup>2</sup>Helmholtz-Zentrum Berlin fuer Materialien und Energie (HZB), Germany

<sup>3</sup>European Organisation for Nuclear Research (Cern), Geneva, Switzerland

<sup>4</sup>Sheffield University, UK

<sup>5</sup>Paul Scherrer Institut (PSI), Villigen, Switzerland

<sup>6</sup>Argonne National Lab (ANL), USA

<sup>7</sup>Illinois Institute of Technology, Chicago, USA

## Abstract

Muon spin rotation ( $\mu$ SR) and point contact tunneling (PCT) are used since several years for bulk niobium studies. Here we present studies on niobium thin film samples of different deposition techniques (diode, magnetron and HIPIMS) and compare the results with RF measurements and bulk niobium results. It is consistently found from  $\mu$ SR and RF measurements that HIPIMS can be used to produce thin films of high RRR. Hints for magnetism are especially found on the HIPIMS samples. These could possibly contribute to the field dependent losses of superconducting cavities, which are strongly pronounced in niobium on copper cavities.

## CURRENT LIMITATIONS OF NIOBIUM ON COPPER CAVITIES

Superconducting cavities prepared by coating a micrometer thick niobium film on a copper substrate enable a lower surface resistance than bulk niobium at 4.5 K the operation temperature of several accelerators using this technology, like the LHC or the HIE-Isolde project. Additionally Nb/Cu cavities have lower material cost, and do not need to be shielded against the earth's magnetic field [1]. Thermal stability is enhanced avoiding quenches [1].

Despite these advantages, the Nb/Cu technology is currently not considered for accelerators requiring highest accelerating gradient  $E_{acc}$  or lowest surface resistance  $R_S$  at temperatures of 2 K and below, because  $R_S$  increases strongly with  $E_{acc}$ . The origin of this field dependent surface resistance has been the subject of many past and recent studies [2–5], but is still far from being fully understood. The film thickness of about 1.5  $\mu$ m is large compared to the London penetration depth  $\lambda_L$  of about 32 nm. Differences in the performance (apart from thermal conductivity issues) should therefore be correlated to the manufacturing procedure and the resulting surface structure. Since no single dominant source can be expected, several hypotheses need

to be addressed individually to identify their origin and possibly reduce their extent.

## Surface Magnetism, a Possible Cause of Dissipation

A possible source of dissipation could be surface magnetism in the oxide layer. Surface magnetism has been found on bulk niobium samples by point contact tunneling [6]. Especially samples cut out from cavity hot spots show strong hints for surface magnetism [7]. This can be correlated to ferromagnetism of nanoparticles in the metal oxides. In Ref. [8] several metal oxid layers were found to have magnetic impurities and ferromagnetism. It was suggested that ferromagnetism is a universal feature of nanoparticles in otherwise nonmagnetic oxides. It is interesting to note that only nanoparticles in the oxides with a size of about 10 nm showed ferromagnetism. If the material was pressed into a bar and sintered the sample became diamagnetic. By sputtering Nb one usually obtains a grain size of several 10 nm, about 2-3 orders of magnitude smaller than fine grain bulk niobium. Nanoparticles could possibly be formed along/between grain boundaries. If they are responsible for dissipation the effect could therefore be a lot stronger for Nb/Cu cavities.

## LE- $\mu$ SR MEASUREMENTS

### Direct Measurement of the London Penetration

Low energy muon spin (LE- $\mu$ SR) rotation enables the measurement of the magnetic field inside a sample as a function of depth. An external magnetic field with a value below  $H_c$  can be applied to probe the London penetration depth of a superconductors as has been done first in 2010 [9] and recently for bulk niobium samples prepared for superconducting cavities [10]. If no external magnetic field is applied LE- $\mu$ SR can be used as a local probe for surface magnetism.

The aim of the  $\mu$ SR experiment presented here was to test whether there are spatial variations in the penetration depth as found in Ref. [10] and/or surface magnetization of niobium thin films on copper substrates prepared by sputter

\* tobi@triumf.ca

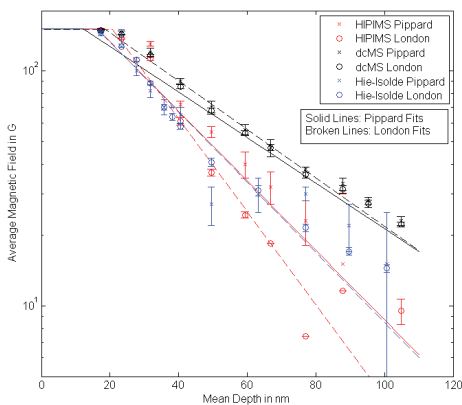


Figure 1: Penetration of the magnetic field in three Nb/Cu samples.

coating. Several coating techniques are presently exploited at CERN; dc Magnetron Sputtering (dcMS), biased diode sputtering (for the Hie-Isolde quarter wave cavities) and High-power Impulse Magnetron Sputtering (HIPIMS). Different microstructures are obtained in each case but all show, unlike bulk material, large field dependent losses. One sample of each technique has been investigated by LE- $\mu$ SR.

Figure 1 shows the obtained penetration profiles obtained from analyzing the LE- $\mu$ SR data using musrfit [11]. Two fit models were used to obtain each data point. A simple Gaussian model based on London theory and a numerical time-domain model based on the non-local Pippard/BCS model [12]. The global Pippard fits have been performed to the whole raw data set. For the HIE-Isolde sample this fit did not converge. Therefore no global Pippard fit is displayed in Fig. 1 for this sample. The deposition here is done in several runs with breaks in between. This might have resulted in an inhomogeneous penetration profile inconsistent with one set of global fit parameters. The penetration depth  $\lambda$  of the dcMS sample is so large that non-local effects become unimportant. The obtained  $\lambda$  is therefore consistent for the local/non-local fit. For the HIPIMS sample, however, non-local effects are more relevant. Clear deviations from the results between local and non-local data analysis were found. Using 1.3 GHz superconducting cavities the penetration depth was also obtained by measuring the frequency shift as a function of temperature for the dcMS and the HIPIMS sample. These values are systematically higher than the values obtained by  $\mu$ SR, see Tab. 1. It should be noted that with RF one only measures the penetration depth change in the temperature range between about 4 and 9 K and obtains  $\lambda$  (0 K) as a fit parameter. Also this method relies on an exponential decay of the magnetic field.

### Zero Field Measurements

Additionally, we have performed zero field measurements in order to search for hints of magnetization at energies of 3.27 and 26.26 keV corresponding to mean muon

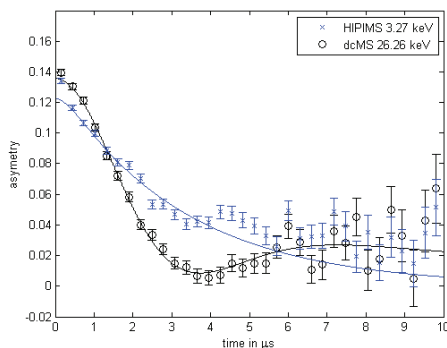


Figure 2: Asymmetry functions obtained at zero field for the HIPIMS sample at the surface and the dcMS sample at about 100 nm depth. The HIPIMS sample shows strong signs of magnetization unlike the dcMS.

stopping depths  $d$  of 17.3 and 104.8 nm for the three samples. The muon spin ensemble depolarization originates from the dephasing of the muon spin in the random dipole field distribution of the nuclear spins [13]. In the presence of static magnetic fields with no muon diffusion, the asymmetry function shows a dip and its value for long times is one third of its maximum. In case of a fluctuating local field or muon diffusion the asymmetry function will deviate from this form; an exponential decay function indicating very strong dynamics [14]. Zero field measurements have been performed in all three samples at the surface and at a depth of about 100 nm. Individual curves have been fitted to a dynamic Gaussian Kubo-Toyabe function [15], characterized by a static width  $\sigma$  and a fluctuation rate  $\nu$ .  $\sigma$  describes the nuclear dipolar broadening, whereas  $\nu$  is describing the dynamics, either due to muon diffusion or magnetic fluctuations. The dcMS and the HIE-Isolde sample show only weak signs of hopping or magnetization, while the HIPIMS sample shows clear signs at both energies, see Tab. 2. Figure 2 shows the two curves with the lowest and highest value of  $\nu$  for illustration. For comparison measurements on bulk niobium samples of different treatments (EP, EP+120C, BCP, N doping) gave very similar  $\nu$  values of around 0.4-0.48 Mhz for all samples [16].

There are three possible explanations for the observed dynamics, muon diffusion, trapped flux or magnetic impurities. A possible measurement to distinguish between the latter two effects is to include zero field measurements above  $T_c$ , which are only sensitive to magnetic impurities. This has been done for the HIE-Isolde sample. The obtained hop

Table 1: Penetration depth value in nm obtained by  $\mu$ SR and RF.  $\mu$ SR results are for local/non-local fit. Error range for RF includes several cavity measurements.

	dcMS	HIPIMS	Hie-Isolde
$\mu$ SR	43(5)/45(2)	22(6)/29(1)	29(5)/-
RF	60(10)	41(9)	-

rates show no significant difference for the superconducting and normal state. Additional measurements above  $T_c$  on the HIPIMS sample are planned. Muon diffusion could be ruled out by growing a  $N_2$  or  $CO_2$  overlayer on the samples and stop the muons in this layer close to the Nb, where the muons are not diffusing, as is also planned for a future experiment.

## PCT ON NIOBIUM FILMS

Point contact tunneling can be used to measure the density of states (DOS) of superconductors. The first application to cavity grade material has been reported in 2008 [6], where it has been shown that cavity grade material has a broadened DOS and a finite zero bias conductance. These findings have been correlated to magnetic impurities in the oxide layer. This has been later confirmed by additional experiments [17]. These studies have then been extended to cut outs from cavity hot and cold spots [7]. The results show that hot spots have a broadened DOS, generally a finite zero bias conductance, some areas with zero bias conductance peaks and more low energy gap values compared to cold spots, which show near ideal tunneling spectra. If these features are related to the Q-slope they should be strongly pronounced in Nb/Cu cavities and samples.

We have tested one sample of each sputtering technique, which were produced simultaneously with the ones used for the  $\mu$ SR experiments presented above. Figure 3 (top) shows the obtained tunneling spectra. For each sample about 80 junctions were measured. The most zero bias peaks are found on the HIPIMS sample, the HIE-Isolde sample has only a few while the dcMS sample has none. One of the zero bias peak junctions on the HIPIMS sample has been measured as a function of temperature, see also Fig. 3. The obtained temperature dependence is consistent with the Kondo effect due to the presence of localized magnetic moments in the oxides or near the interface as has been earlier reported for a bulk niobium sample [17]. The obtained gap values are extracted from fits of the conductance curves to the Blonder-Tinkham-Klapwijk (BTK) model [18, 19], see Fig. 3 (middle). The dcMS sample has the least sub gap junctions, while the HIE-Isolde sample has the most. The

Table 2: Fluctuation rate  $\nu$  and static width  $\sigma$  of three Nb/Cu samples for different temperatures  $T$  and mean muon stopping depths  $d$

Sample	$d$ [nm]	$T$ [K]	$\nu$ [MHz]	$\sigma$ [ $\mu$ s $^{-1}$ ]
HIPIMS	17.3	3.75	$3.0 \pm 2.2$	$0.65 \pm 0.16$
	104.8	3.83	$4.2 \pm 2.1$	$0.71 \pm 0.27$
dcMS	17.3	3.30	$0.43 \pm 0.05$	$0.49 \pm 0.03$
	104.8	3.55	$0.11 \pm 0.03$	$0.50 \pm 0.012$
Hie-Isolde	17.3	2.70	$0.34 \pm 0.04$	$0.51 \pm 0.011$
	17.3	11.00	$0.52 \pm 0.07$	$0.47 \pm 0.014$
	100.0	2.66	$0.28 \pm 0.03$	$0.429 \pm 0.008$
	100.0	10.84	$0.31 \pm 0.03$	$0.500 \pm 0.008$

broadening of the DOS is directly apparent from the tunneling spectra displayed on top of Fig. 3. To quantify this feature the BTK fits include the phenomenological quasiparticle lifetime broadening parameter  $\Gamma$ . The lower its value the sharper the density of states, the less there is inelastic quasiparticle scattering. In Fig. 3 (bottom)  $\Gamma$  is displayed for the three samples. The distribution of the values is similar for the dcMS and the HIPIMS sample peaking at approx 0.1 mV. For the HIE-Isolde sample most junctions have lower  $\Gamma$  values. The distribution is however less homogeneous including more junctions with  $\Gamma > 0.2$  mV.

## How Hot Spots from Low Energy Gaps Cause Q-slope

The samples investigated here, as well as hot spots cut out from bulk niobium cavities show several features in the tunneling spectra, while cold spots resemble more the ideal tunneling spectra [7]. In order to use PCT as a predictive tool for cavity performance each of these features needs to be correlated to RF measurements. In the following a short phenomenological explanation how areas with a lowered superconducting gap will affect the overall surface resistance and the Q-slope is given. The surface resistance is exponentially higher for lower gap values since  $R_S \propto \exp(-\Delta/k_b T)$ . The following considerations are inspired by the model for thermal breakdown from Ref. [20]. Assume there is a small hemispherical defect on the surface with lowered  $\Delta^*$  of radius  $a$ . The power dissipation by this defect will be

$$P = \frac{1}{2} R_S^* H^2 \pi a \quad (1)$$

with a surface resistance

$$R_S = A f^2 \frac{e^{(-\Delta^*/k_b T_a)}}{T_a}, \quad (2)$$

including the parameter  $A$ , which depends on the material properties. When the problem is changed to a spherical defect surrounded by niobium with thermal conductance  $\kappa$  and full gap value as described in [20] one can calculate the heat flow  $t$  and from this the temperature  $T_a$  of the defect.

$$T_a = T_b + \frac{H^2 a A f^2 \frac{T_c}{T_a} \exp(-\Delta^*/k_b T_a)}{4\kappa}. \quad (3)$$

With increasing field the area around the sub gap state will heat up expanding to areas with the full gap values. A localized thermal feedback is induced, creating hot spots. These areas will have a larger surface resistance

$$R_S = A f^2 \frac{e^{(-\Delta/k_b T_a)}}{T_a}. \quad (4)$$

The surface resistance of the material with full gap value around a defect with reduced gap value will be field dependent. This can be shown by solving equations 3 and 4 numerically. Figure 4 displays results for two values of  $\Delta/\Delta^*$ . A defect size radius  $a$  of 100  $\mu$ m was assumed. The area

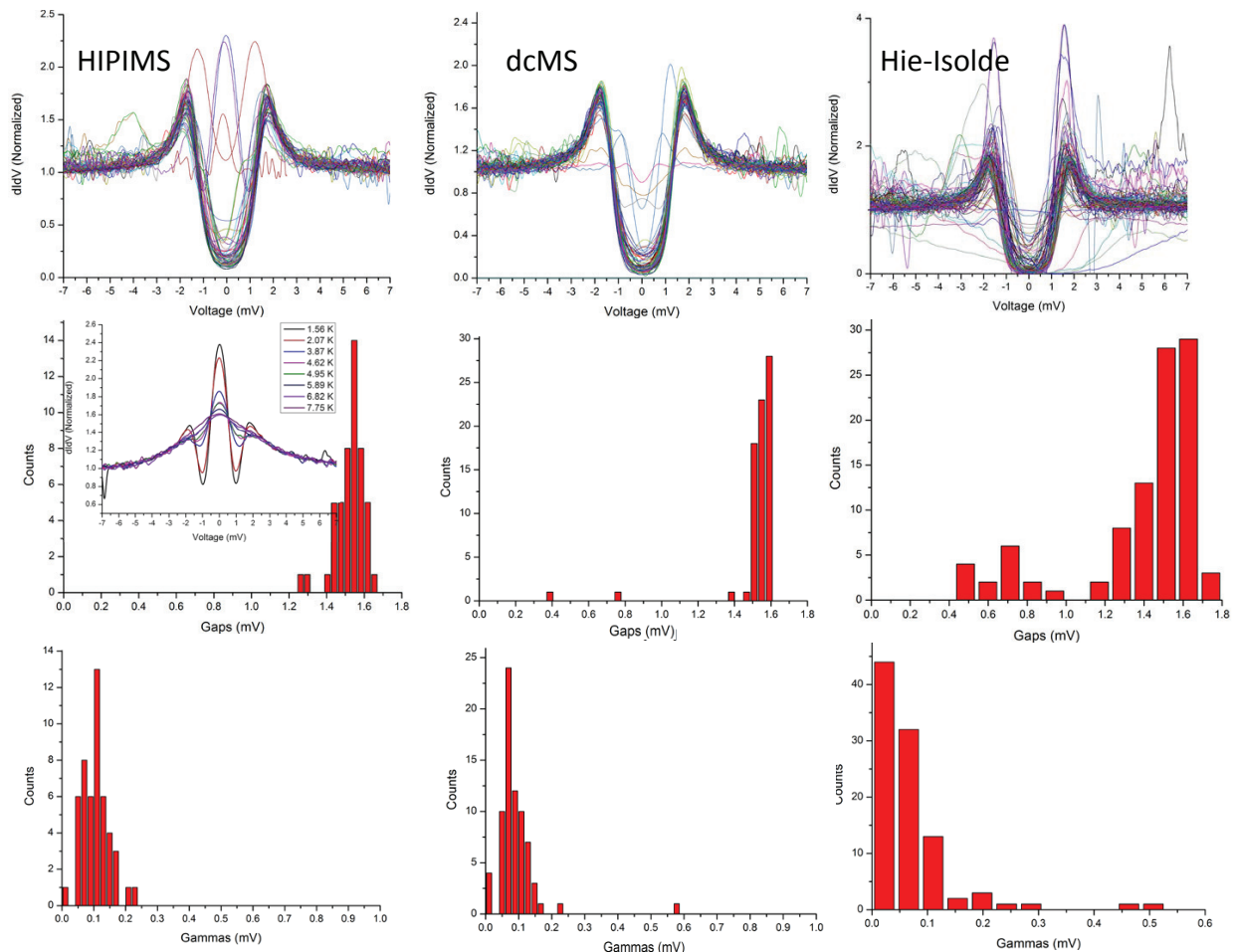


Figure 3: Tunneling spectra of about 80 junctions each for three Nb/Cu samples (top). Corresponding gap values (middle) and phenomenological quasiparticle lifetime broadening parameter  $\Delta$  (bottom). Inset middle left: Conductance of a zero bias peak on the HIPIMS sample as a function of temperature.

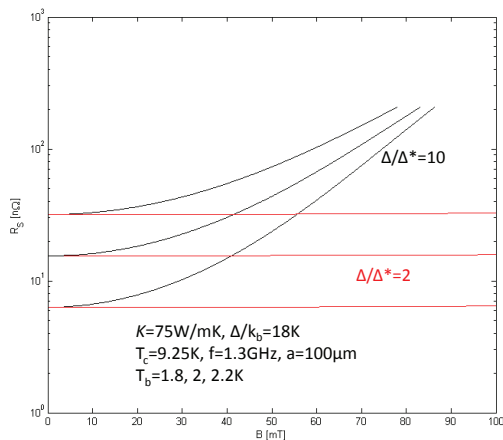


Figure 4: Surface resistance of the area around a defect with suppressed gap value as a function of applied magnetic field.

over which a sub gap state is extended is unknown. A lower estimate is the tip size of the PCT system of  $100 \mu m^2$ . The

PCT setup includes a piezo stage which can be used to estimate this area in future measurements. In any case the area of the sub gap state is large compared to the size of single magnetic nanoparticles which we propose to be a cause of dissipation. Therefore only extended areas of a larger density of magnetic nanoparticles in hot spots are consistent with our model. According to this very simplified model only sub gap states with very low  $\Delta^*$  contribute significantly to the Q-slope. The effect will become stronger when the areas with suppressed gap values quench. This could possibly be related to the Q-drop at high field. There is no general relationship between the energy gap and the RF critical field. It is however reasonable to assume that a lowered energy gap results in a lowered critical RF field.

The simple model introduced here is consistent with the finding that hot spots unlike cold spots cutout from cavities show sub gap states [7]. We see that PCT can indeed be used as a predictive tool for cavity performance. Sub gap states might be a reason why Nb/Cu cavities have a stronger Q-slope than cavities from bulk material. Localized heating as the cause of Q-slope is also consistent with the recent



finding that the overall inner surface temperature of a HIP-IMS Nb/Cu cavity was heating up far below what one would expect for global thermal feedback [5]. In order to further investigate the effect of sub gap states on the performance of Nb/Cu cavities we propose to perform temperature mapping and PCT on cold and hot spot cut outs from Nb/Cu cavities.

## CONCLUSION

It has been shown how sub gap values as measured with PCT can have a direct influence on the Q-slope of superconducting cavities by creating hot spots. For bulk niobium it has been shown in [21] that sub gaps states can be suppressed by high temperature baking. For Nb/Cu cavities such a treatment is not possible due to the lower melting temperature of copper. The origin of the Q-slope of Nb/Cu might be related to magnetic nanoparticles in the oxide layer and possibly between grain boundaries. Magnetic impurities can severely decrease the energy gap of superconductors as has been shown in [22]. The presence of magnetic impurities is supported here for the HIPIMS sample by LE- $\mu$ SR zero field measurements.

## ACKNOWLEDGMENT

The authors thank Alban Sublet (CERN) for the preparation of the Hie-Isolde samples. The  $\mu$ SR measurements were performed at the Swiss Muon Source (S $\mu$ S), at the Paul Scherrer Institute in Villigen, Switzerland. This work has been funded partly by a Marie Curie International Outgoing Fellowship and the EuCARD-2 project of the European Community's 7th Programme and by the U.S. Department of Energy, Office of Sciences, Office of High Energy Physics, early Career Award FWP 50335 and Office of Science, Office of Basic Energy Sciences under Contract No. DE-AC02-06CH11357.

## REFERENCES

- [1] S. Calatroni. 20 Years of experience with the Nb/Cu technology for superconducting cavities and perspectives for future developments. *Physica C: Superconductivity*, 441:95 – 101, 2006.
- [2] C. Benvenuti et al. Study of the surface resistance of superconducting niobium films at 1.5 GHz. *Physica C*, 316, 1999.
- [3] C. Benvenuti et al. CERN studies on niobium-coated 1.5 GHz copper cavities. In *The 10th Workshop on RF Superconductivity, 2001, Tsukuba, Japan*, 2001.
- [4] S. Calatroni et al. Progress of Nb/Cu technology with 1.5 GHz cavities. In *Proceedings of the 11th Workshop on RF Superconductivity, Luebeck/Travemuende, Germany*, 2003.
- [5] T. Junginger. Field dependent surface resistance of niobium on copper cavities. *Phys. Rev. ST Accel. Beams*, 18(7):072001, 2015.
- [6] T. Proslie et al. Tunneling study of cavity grade Nb: Possible magnetic scattering at the surface. *Appl. Phys. Lett.*, (92):212505, 2008.
- [7] C. Cao et al. Probing hot spot and cold spot regions of SRF cavities with tunneling and Raman spectroscopies. In *Proceedings of SRF2013, Paris, France, TUP019*, 2013.
- [8] A. Sundaresan et al. Ferromagnetism as a universal feature of nanoparticles of the otherwise nonmagnetic oxides. *Phys. Rev. B*, 74:161306, 2006.
- [9] T. J. Jackson et al. Depth-Resolved Profile of the Magnetic Field beneath the Surface of a Superconductor with a Few nm Resolution. *Phys. Rev. Lett.*, 84(21):4958, 2000.
- [10] A. Romanenko et al. Strong Meissner screening change in superconducting radio frequency cavities due to mild baking. *Appl. Phys. Lett.*, 104:072601, 2014.
- [11] A. Suter and B.M. Wojek. Musrfit: A Free Platform-Independent Framework for muSR Data Analysis. *Physics Procedia*, 30:69–73, 2012.
- [12] A. Suter et al. Observation of nonexponential magnetic penetration profiles in the Meissner state: A manifestation of non-local effects in superconductors. *Phys. Rev. B*, 72:024506, 2005.
- [13] A. Yaouanc and P. Dalmas de Reotier. *Muon Spin Rotation, Relaxation, and Resonance*. Oxford University Press 2011, 2011.
- [14] R. S. Hayano et al. Zero- and low-field spin relaxation studied by positive muons. *Phys. Rev. B*, 20(3):850, 1979.
- [15] A. Schenck. *Muon Spin Rotation Spectroscopy: Principles and Applications in Solid State Physics (Adam Hilger, England, 1985)*, pp. 83-87.
- [16] A. Romanenko. Private communication.
- [17] T. Proslie et al. Evidence of Surface Paramagnetism in Niobium and Consequences for the Superconducting Cavity Surface Impedance. *IEEE Transactions on Applied Superconductivity*, 21(3):2619, 2011.
- [18] C. Dynes, V. Narayanamurti, and J. P. Garno. Direct Measurement of Quasiparticle-Lifetime Broadening in a Strongly-Coupled Superconductor. *Phys. Rev. Lett.*, 41:1509, 1978.
- [19] G. E. Blonder, M. Tinkham, and T. M. Klapwijk. Transition from metallic to tunneling regimes in superconducting microconstrictions: Excess current, charge imbalance, and supercurrent conversion. *Phys. Rev. B*, 25:4515, 1982.
- [20] Hasan Padamsee, Tom Hays, and Jens Knobloch. *RF superconductivity for accelerators*. Wiley, Weinheim, 2. edition, 2008.
- [21] P. Dhakal et al. Effect of high temperature heat treatments on the quality factor of a large-grain superconducting radio-frequency niobium cavity. *Physical Review Special Topics - Accelerators and beams*, 16:042001, 2013.
- [22] F. Reif and A. Woolf. Energy Gap in Superconductors containing Paramagnetic Impurities. *Phys. Rev. Lett.*, 9(7):315, 1962.